π - pulse

January 22, 2019

Contents

1 Controlling the interparticle interactions in a correlated electron system

Studying the interparticle interactions in a correlated electron system by applying laser pulses is a challenging perspective, which may lead to some states of matter that do not exist in equilibrium. For example, changing the electron-electron interaction from the original Coulomb repulsion to an attraction, can induce an s-wave superconducting state with very high transition temperature,1,2 or the BCS-BEC crossover.2,3

Creation a population inversion in metallic bands corresponding to a negative temperature (T) state.9,10 is one of the way to control the interaction. Such investigation done in work of Tsuji et al. [2012] for hipercubic lattice, where was shown that it is possible to induce a population inversion in metallic systems using a properly shaped half-cycle or monocycle pulses, the system without energy dissipation will thermalize in the negative T state after the pulse. This implies an effective switching of the interaction from repulsive to attractive, since a density matrix $\exp(-H/T)$ for a Hamiltonian H with temperature $T < 0$ corresponds to the one for the inverted $-H$ with $-T > 0$.11,12

Effective switching of the interaction from repulsive to attractive occur because a density matrix $\exp(-H/T)$ for a Hamiltonian H with temperature $T < 0$ corresponds inverted $-H$ with $-T > 0$.

1.1 Creation of population inversion by linear polarized electric field

In this chapter we repeat work Tsuji et al. [2012] taking realistic 2d square lattice and focused in transient nonequilibrium dynamics with different polarization of electric field.

By the half-cycle pulse we induce shift in the momentum distribution of the electrons. Selecting the parameters of such a pulse we can achieve half of the Brillouin zone, the system is brought to a negative-T state, this is often (depending on the value of the interaction) leads to change of the interaction from repulsive to attractive.

1.1.1 Half-cycle vector potential

To investigate effects of negative temperature state we use single-band Hubbard model driven by an half-cycle electric field. Half-cycle pulse chosen in Y and diagonal directions to look polarisation dependence and iverson of population.

The vector potential has the form:

$$A(t) = \frac{A_{max}}{\tau}(t - \tau sin(2\pi t/\tau)) \tag{1}$$

where A_{max} - amplitude of vector potential; τ - pulse length.

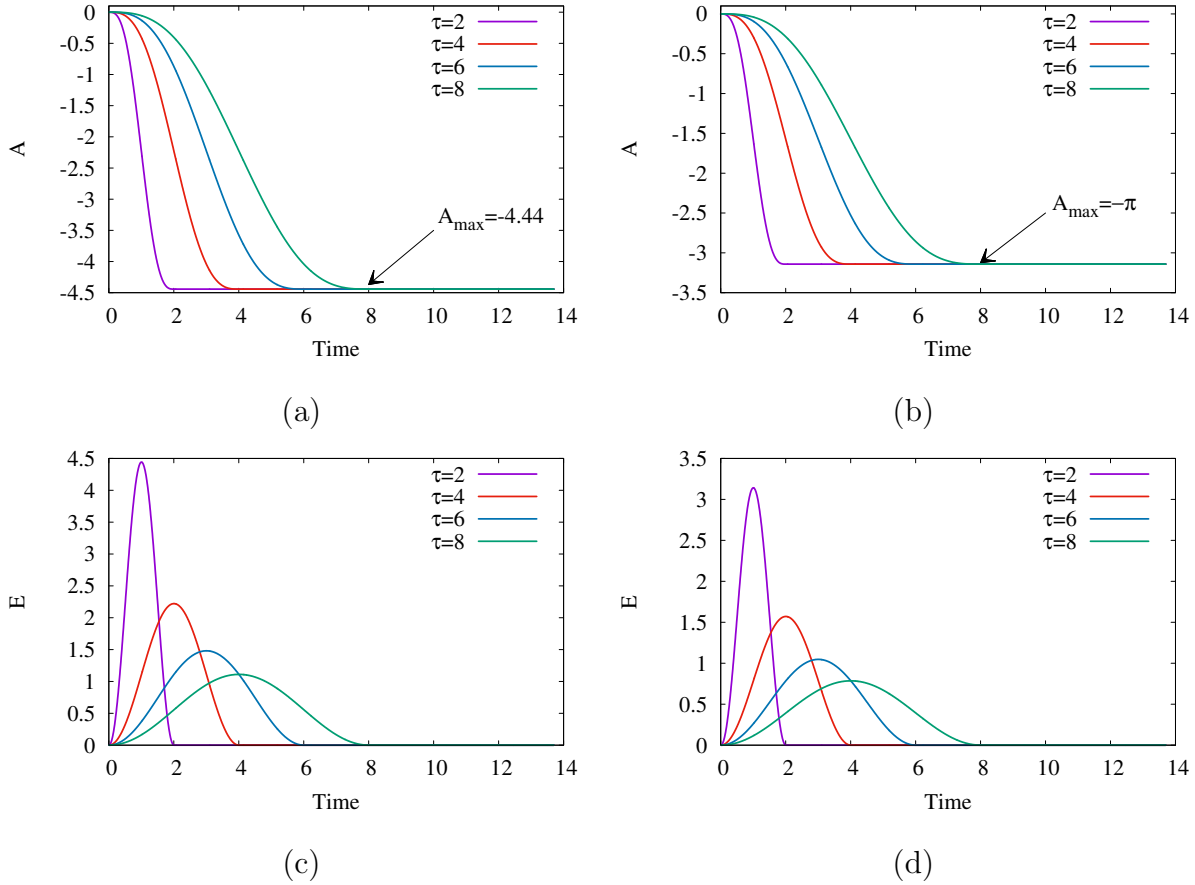

Figure 1: Vector potential and external electric field: a,c for diagonal direction; b,d for Y direction

In case Y direction of field, the maximum value of the vector potential $A_{max} = \pi$ (Figure 1a,c). For diagonal direction of field the maximum value of the vector potential $A_{max} = \pi * \sqrt{2}$ (Figure 1b,d). This allows to shift the momentum distribution in the case of Y-field from Γ to Y, in the case of diagonal field from Γ to M in the Brillouin zone.

1.1.2 Total energy and double occupancy.

From the total energy we can recognize the repulsion-to-attraction transition. After the pulse excitation isolated system is supposed to approach a thermalized state [25] with some effective temperature T_{eff} and a total energy E_{tot}. A thermal state with a

positive temperature has $E_{tot} < 0$ for the interaction term of the Hamiltonian at half filling, while $E_{tot} > 0$ happens at negative temperature. Thereby the total energy is an order parameter for the repulsion-to-attraction transition. Suchwise if $E_{tot} > 0$ the system arrives at a negative temperature state ($T_{eff} < 0$) Tsuji et al. [2012].

To show effect of inversion population we choose half-cycle shape of electric field with $\tau = 4$ (red line in Figures 1c,d) and investigate behaviour of total energy and double occupancy (Figure 2).

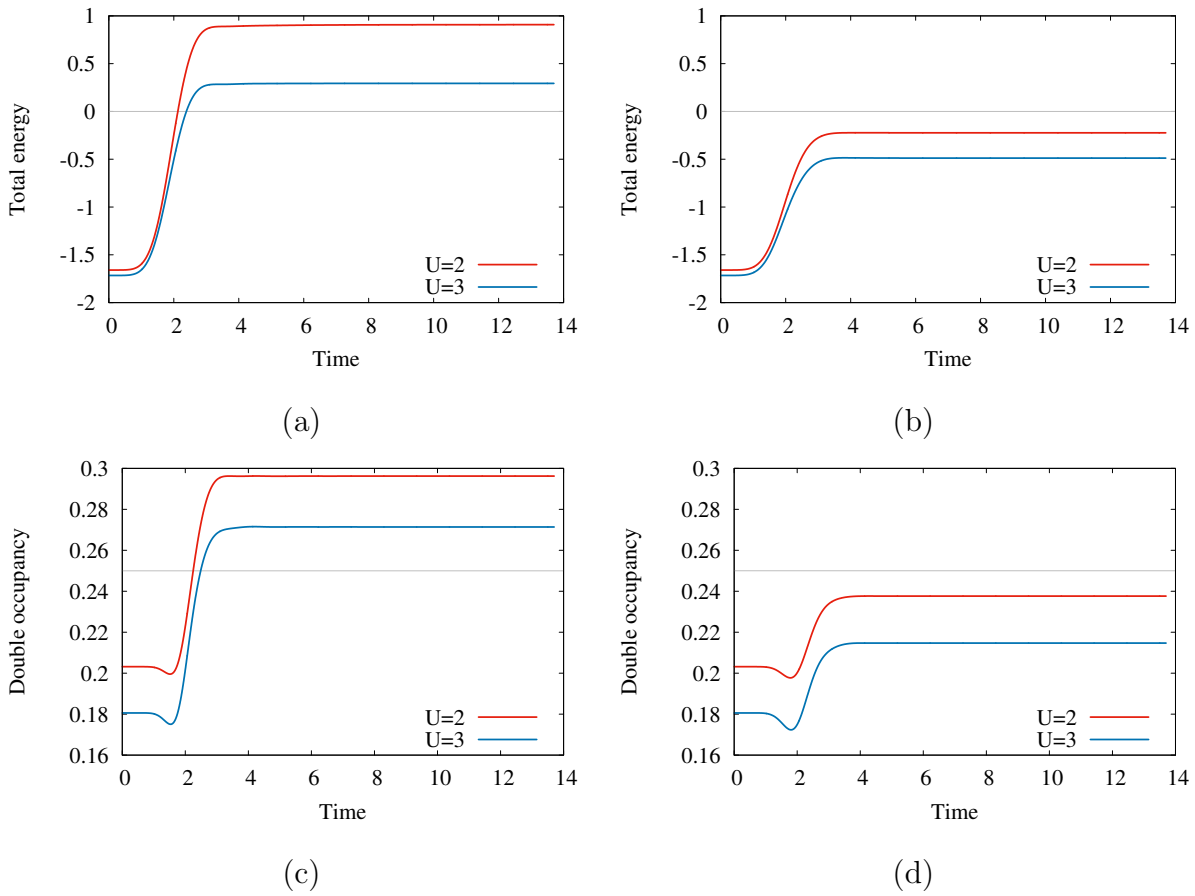

Figure 2: Total energy and double occupancy ($\tau = 4$): a,c for XY direction of pulse ($A_{max} = \pi\sqrt{2}$); b,d for Y direction of pulse ($A_{max} = \pi$).

From analysis of Fig. 2 we can observe a change in the sign of the interaction in case of field in the diagonal direction, U=2 and U=3. $E_{tot} > 0$ (the total energy has the origin at zero) and double occupancy $docc > 0.25$ after the pulse. It seen then lower Coulomb interaction than E_{tot} has bigger value and more pronounced effect of negative temperature state after pulse. In case of Y direction of electric field total energy negative all the time so the interaction does not change the sign.

In Figure 3 is shown total energy after the pulse for $\tau = 4$ as a function of the magnitude of the vector potential for diagonal and Y field directions. The graph shows that for the field in the diagonal direction there is a positive total energy which means that the sign of interaction has changed. The value of the total energy is maximum when the value of the amplitude of the vector potential such that exactly shift momentum distribution in the case of Y-field from Γ to Y and in the case of diagonal field from Γ to M in the Brillouin zone. As the magnitude of the vector potential decreases, the total energy decreases and, for a certain value of the vector potential, the total energy becomes negative. This is in accordance with the results of article Tsuji et al. [2012]. When the interaction increased, the value of the total energy decreases and the range of values of the total energy for the different amplitudes of the vector potential. In Y-direction of the

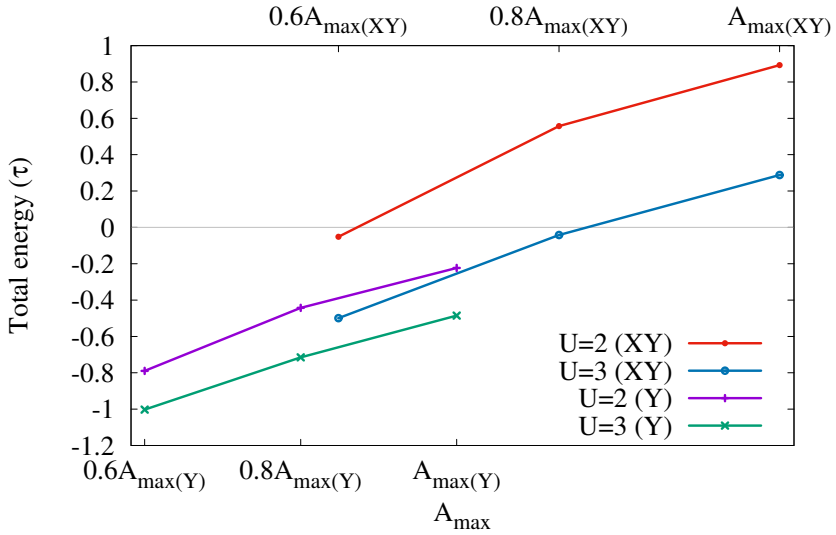

Figure 3: The total energy after the pulse as a function of the magnitude of the vector potential ($\tau = 4$).

field, there is no change in the sign of the interaction with different values of the vector potential and the Coulomb interaction (U=2,3).

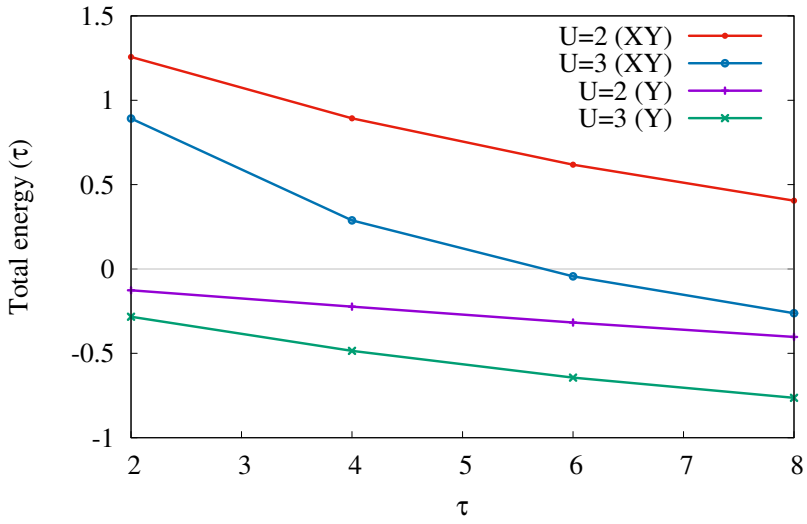

Figure 4: The total energy after the pulse as a function of the pulse width.

The total energy after the pulse ($A_{max} = \pi$ Y-field; $A_{max} = \pi\sqrt{2}$ XY-field) as a function of pulse width depicted in Figure 4. It can be seen from the figure that for a pulse with $\tau = 2$ (XY field direction), the total energy has a positive and maximum value (red and blue lines), this pulse narrowest in the calculations. With increasing pulse width, the total energy after the pulse can become negative, as seen on the blue line. This behavior was demonstrated also in the work [Tsuji et al. [2012]] for hypercubic lattice. In the case of a pulse in the Y-direction, the total energy is always negative. With increasing pulse width the total energy goes to a more negative region.

1.1.3 Momentum distribution. A_{max}-pulse.

Visually change of electron population can be traced in time-dependent momentum distribution. This part shows the momentum distribution and how it varies with time under the action of half-cycle cosine pulse.

The Figure 5 shows momentum distribution of the interacting system (U=2) at time $t = 0$ when the system is in equilibrium and the field does not act on it. The maximum of the momentum distribution is at the Γ-point and the minimum at the angles of the first Brillouin zone.

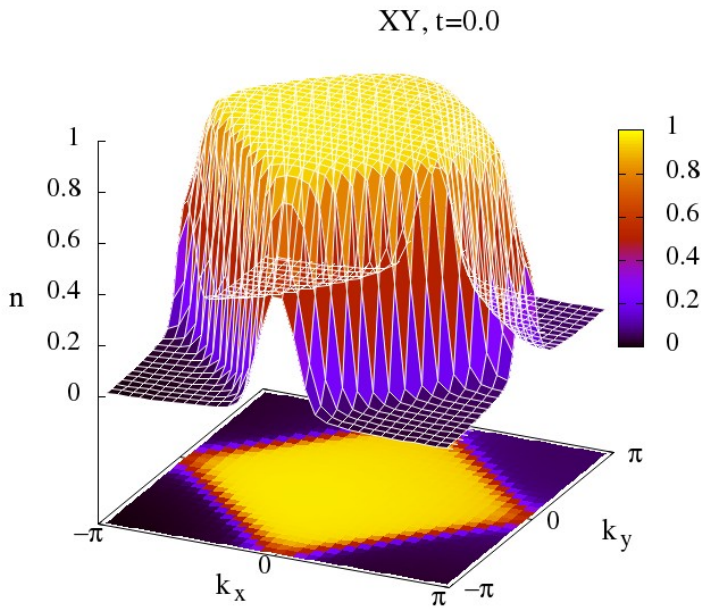

Figure 5: Equilibrium momentum distribution for U=2 at time=0.

When the field is turned on, momentum distribution begins to move in the direction of the vector potential (or opposite to the direction of the electric field).

In Figure 6 shown momentum distribution for U=2 during the action of the pulse. The pulse exists at time 0 to 4 ($\tau = 4$). In the diagonal direction of the field (Figure 6a,c,e), the shift and flattening of the momentum distribution are seen. This shift leads to inversion of the population, since the maximum of the momentum distribution at the final instant of time (t=4) is at the corners of the first Brillouin zone and the minimum at the Γ-point. This finite distribution does not change much after the pulse (Figures 7a,c,e). Also on (Figure 2a) seen that after the pulse the total energy is positive.

For a field in Y-direction there is no population inversion (Figures 6b,d,f). Under the influence of the field, it also shifts to the value of the vector potential. For the Y-direction momentum distribution has a long relaxation time (Figures 7b,d,f) in comparison with the XY-direction (Figures 7a,c,e).

In Figure 8 is shown momentum distribution for U=3 during the action of the pulse. In the diagonal direction of the field (Figure 8a,c,e), the shift and flattening of the momentum distribution are seen. This shift leads to inversion of the population. Distribution after exitation does not change (Figures 9a,c). In Figure 2a seen that after the pulse the total energy is positive but less than in the case of U=2.

For a field in Y-direction there is no population inversion (Figures 8b,d,f). Under the influence of the field, it also shifts to the value of the vector potential. For the Y-direction momentum distribution has a short relaxation time (Figures 9b,d).

Thus, as the interaction is increased so that the momentum distribution becomes flatter for all directions. This can be associated not only with correlation effects which together with the electric field change the topology of the momentum distribution, but also with an increase in the effective temperature of the system.

Increasing the value of the Coulomb interaction reduces the relaxation time of the

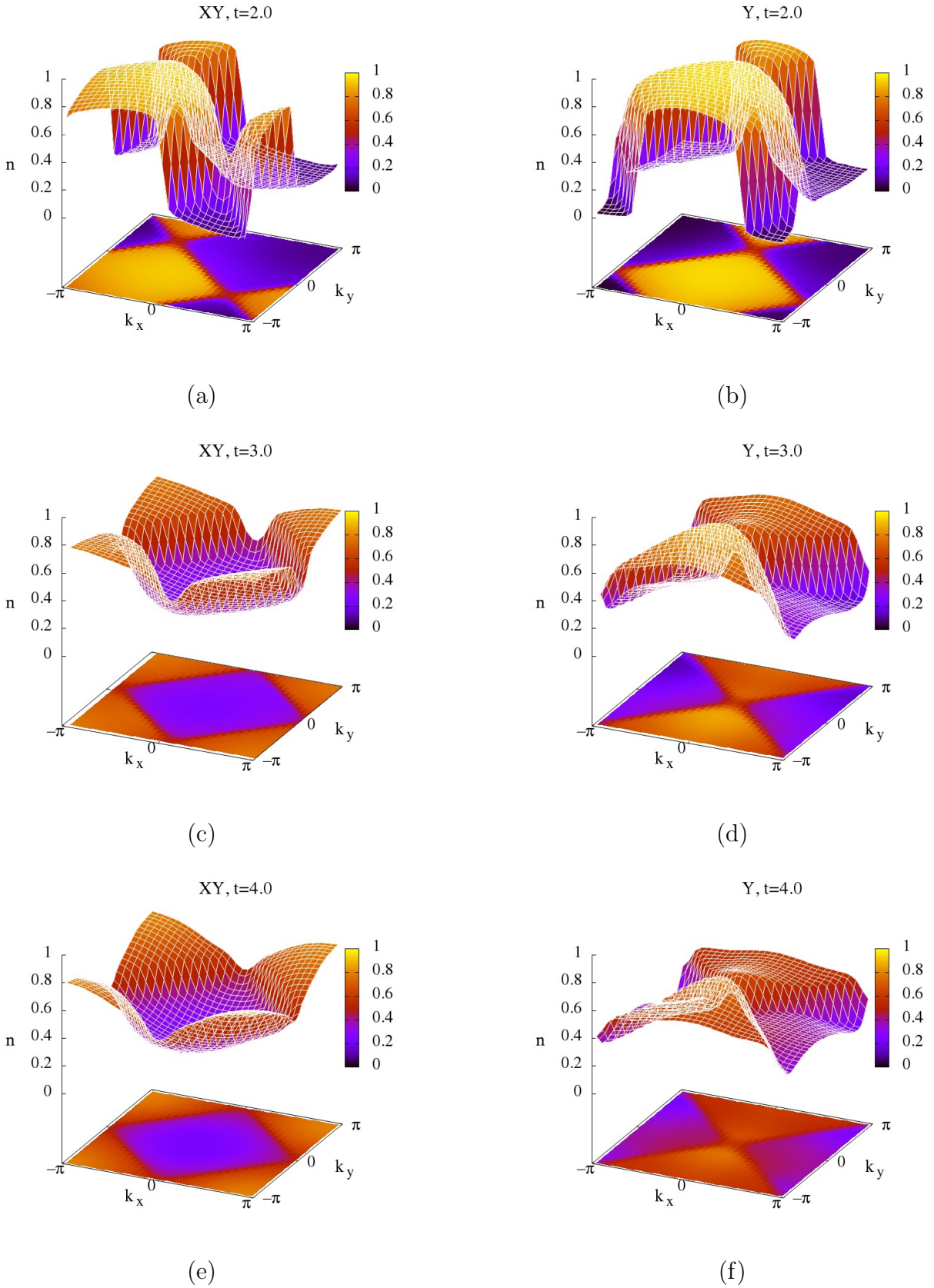

Figure 6: Momentum distribution for U=2 at different times (from 2 to 4), τ=4. Left column a,c,e - field in XY direction; right column b,d,f - field in Y direction.

distribution after radiation. This is clearly seen in comparing the results of relaxation for the Y direction of the field for different values of the interaction.

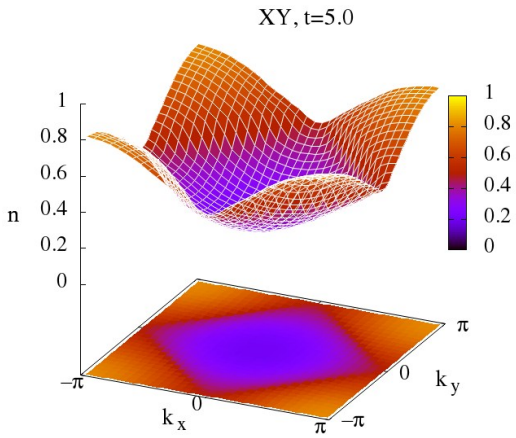

(a)

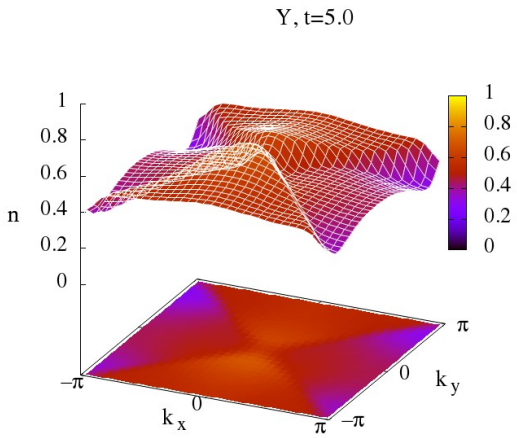

(b)

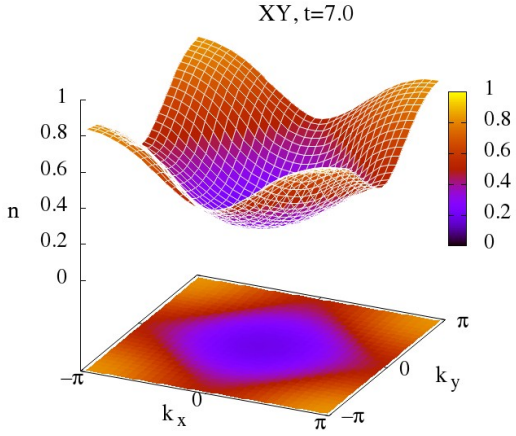

(c)

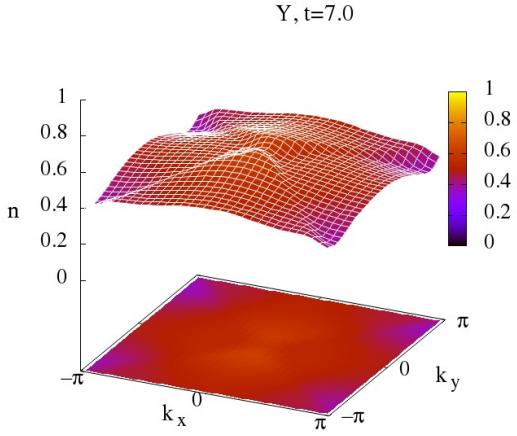

(d)

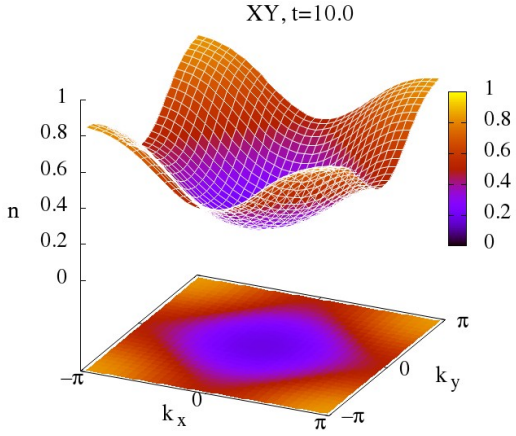

(e)

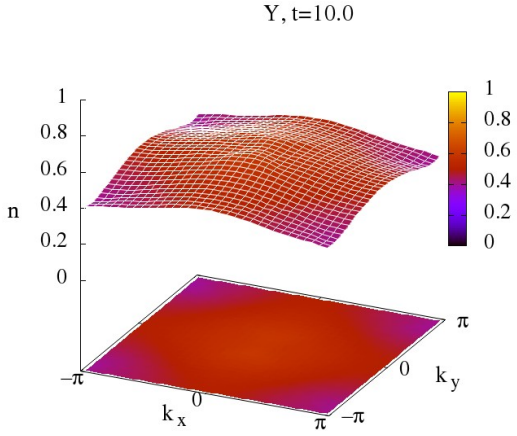

(f)

Figure 7: Relaxation of momentum distribution (after pulse) for U=2 in different times (from 5 to 10), τ=4. Left column a,c,e - field in XY direction; right column b,d,f - field in Y direction.

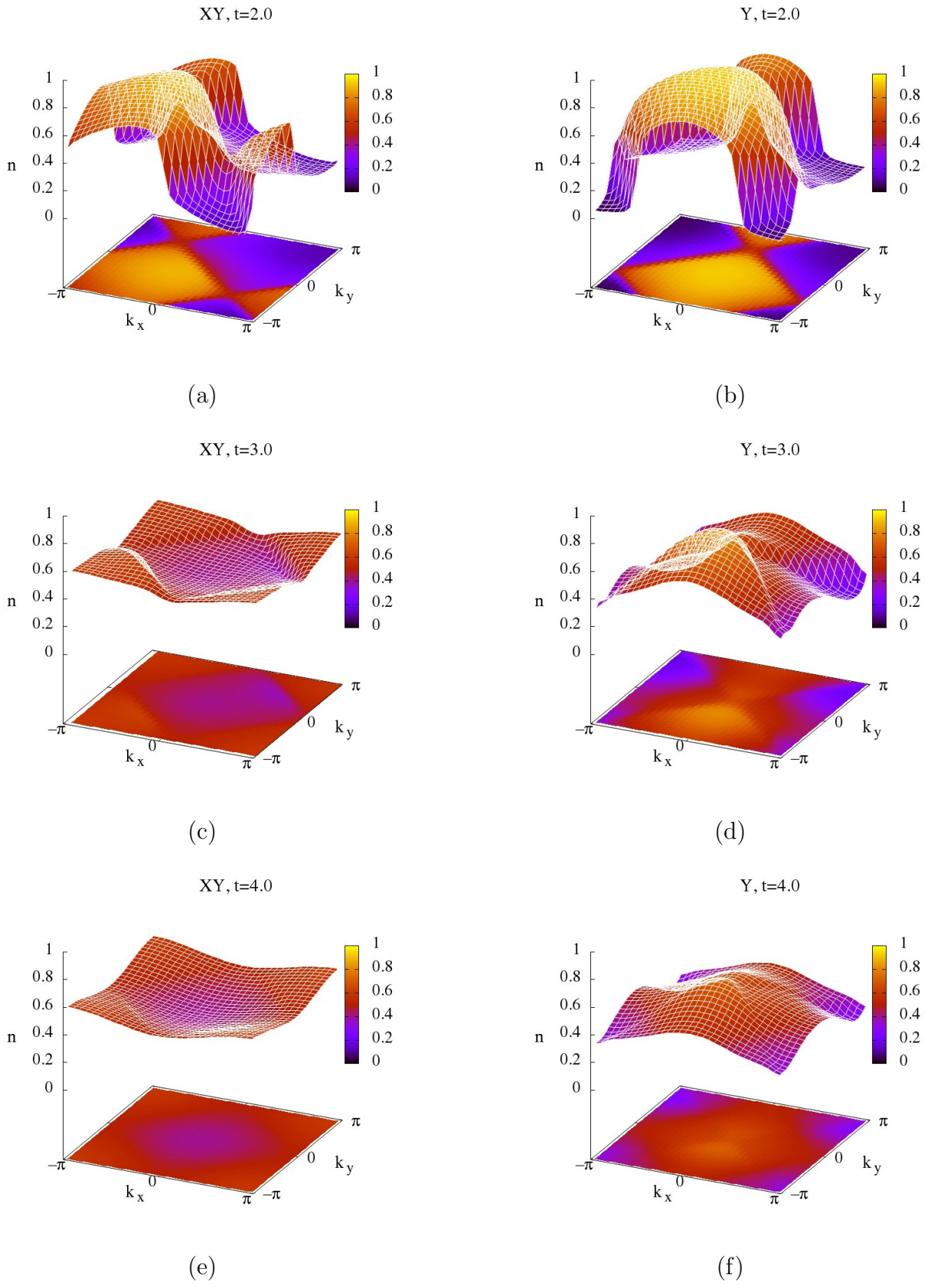

Figure 8: Momentum distribution for U=3 in different times (from 2 to 4), τ=4. Left column a,c,e - field in XY direction; right column b,d,f - field in Y direction.

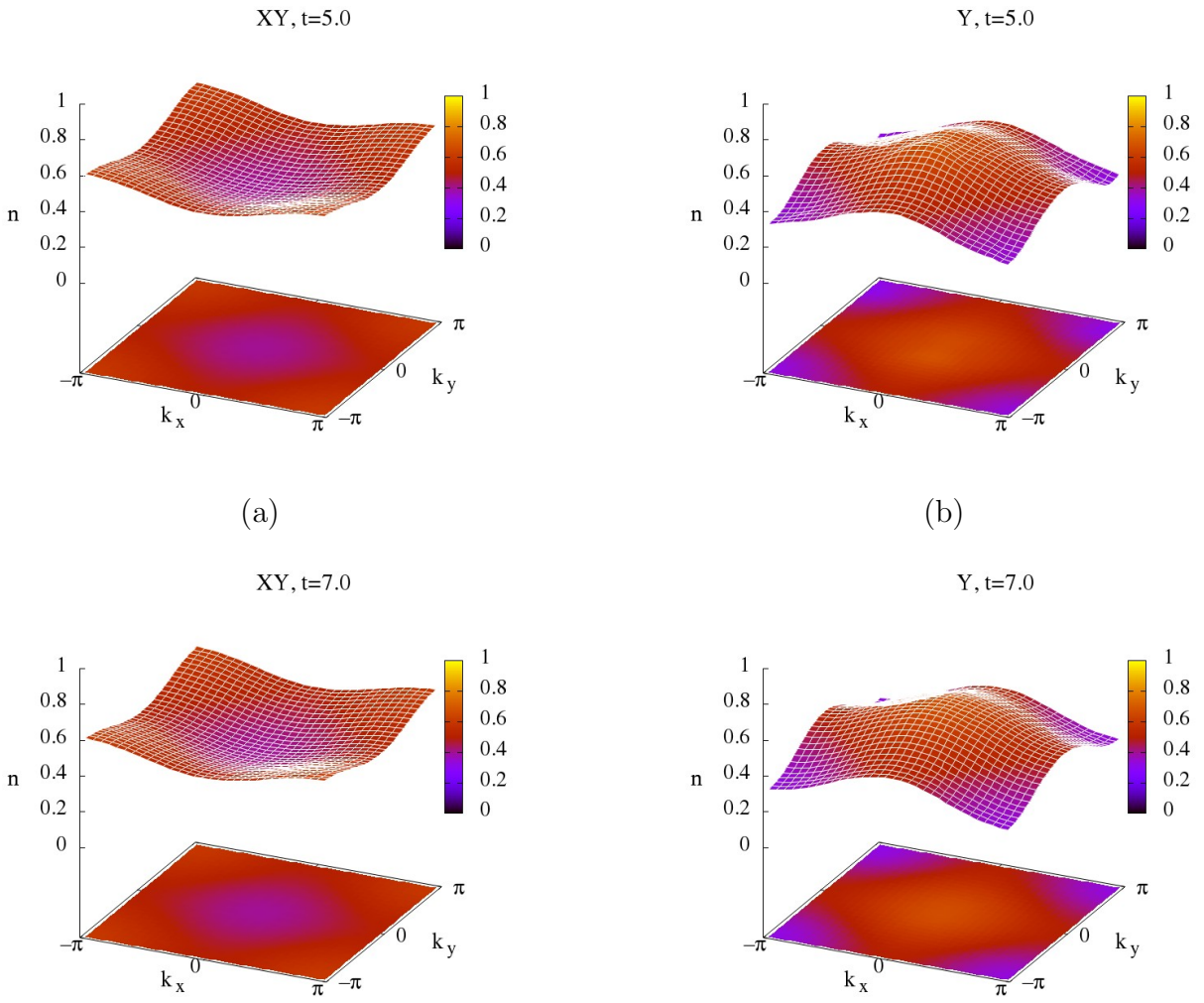

Figure 9: Relaxation of momentum distribution (after pulse) for U=3 in times 5 and 7, τ=4. Left column a,c - field in XY direction; right column b,d - field in Y direction.

1.1.4 Momentum distribution. $0.8A_{max}$-pulse.

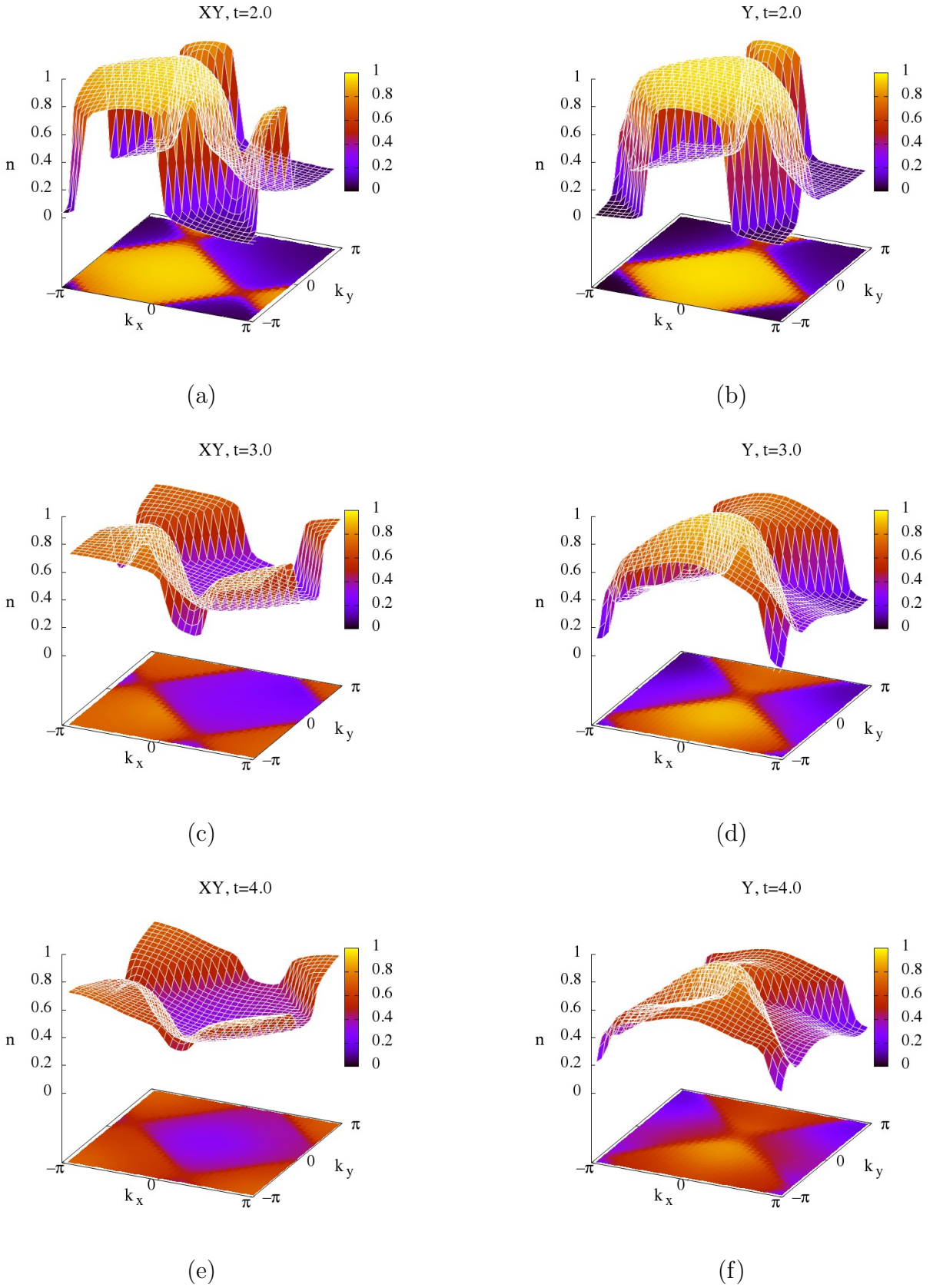

Figure 10: Momentum distribution for U=2 in different times (from 2 to 4), τ=4. Left column a,c,e - field in XY direction; right column b,d,f - field in Y direction.

In Figures 10 and 11 is shown momentum distribution for U=2 during the action of the pulse and relaxation. There were used a pulses with $0.8A_{max}$. This do not allows to

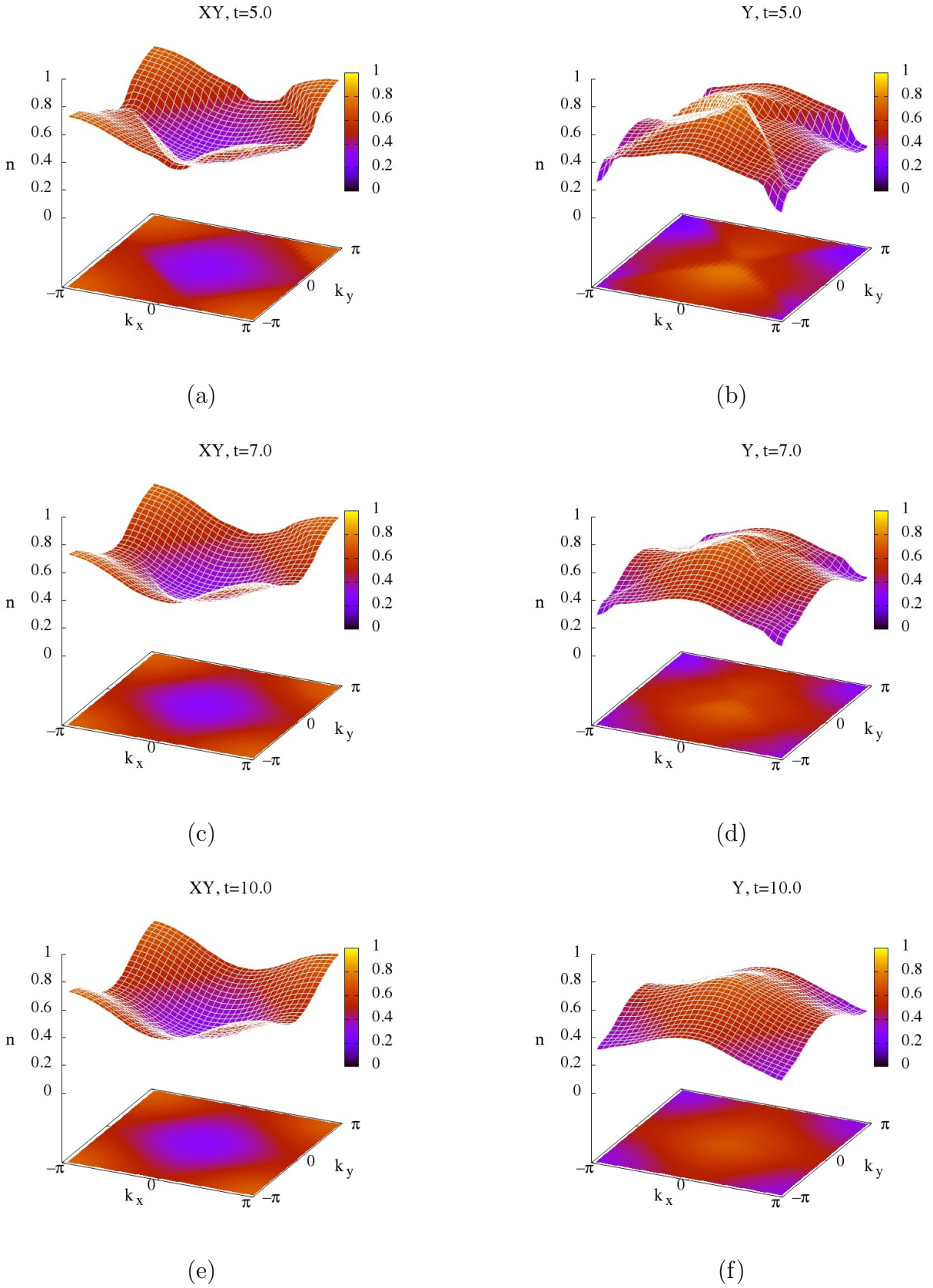

Figure 11: Relaxation of momentum distribution (after pulse) for U=2 in different times (from 5 to 10), τ=4. Left column a,c,e - field in XY direction; right column b,d,f - field in Y direction.

shift the momentum distribution in the case of Y-field from Γ to Y during excitation, in the case of diagonal field from Γ to M in the Brillouin zone during the pulse. This can be seen in the Figures 10e,f, these are the graphs of the momentum distribution in which

the pulse end.

In the process of relaxation Figures 11a,c,e, the minimum of the momentum distribution shifted to the Γ point for diagonal field. It take place because the system needs to adjust the momentum shift to $\pi\sqrt{2}$ to achieve a thermal state. The distribution relax to thermal states with $T_{eff} < 0$. As expected, field in Y direction does not turn over distribution of electrons (Figure 11b,d,f). Effect of shifting to the Γ point of maximum population exist to reach a thermal state.

Geometry of 2D square lattice give us possibility to investigate polarization dependence of physical quantity. Due to this, the behavior of the system under the action of a linearly polarized fields in the diagonal and Y direction was considered.

In the case of a diagonal field, many effects have been found which in agreement with the article Tsuji et al. [2012] such as population inversion, behaviour of relaxation of the momentum distribution to the thermal state in case of non optimal vector potential.

For Y field direction population inversion is not observed at the considered parameters of the laser pulse and the Coulomb interaction. This is seen in the graphs of the total energy, double occupancy and the momentum distribution. Distribution has a long relaxation time compared with the results for the diagonal field direction.

It is important to note how the parameters of the system and the pulse separately affect the distribution. In equilibrium, correlations and temperature blur Fermi step, the electric field used as a vector potential simply shifts the distribution by the value of this vector potential. In nonequilibrium in the absence of correlations, the momentum distribution moves in the direction of the vector potential without changing its shape. A common effect in both directions of the field is the distortion of the momentum distribution under the action of the combined effects of correlations, the electric field and an increase of the effective temperature.

1.2 Change the sign of the interaction using a circularly polarized field

We continue investigate situation when system has change of sign of interaction. In this part we focused in behaviour of the single-band Hubbard model under circularly polarized vector potentials on a 2D square lattice.

Selecting the parameters of a pulse possible to change of the interaction from repulsive to attractive by different scenarios. As noted earlier, the most popular way to change the population in this section will be transferring the middle point of the momentum distribution, which is located in the Γ point of the first Brillouin zone initially before pulse, to the M point. For this purpose we use a half- mono- and multi-cycle pulses with different shape and phase parameters.

1.2.1 Polarization dependence of the circular π-pulse

Consider the transition from linear to circular polarization for half-cycle pulse. Figure 12 shows the graphs of vector potentials. Pulse parameters are written in the Table 1.

The trajectory of the center of momentum distribution is shown in Figure 13. As we can see, this trajectory strongly depends on the polarization and the amplitude of the vector potential. The curves with an initial phase equal to $\phi_y = \pi/4$ corresponds to circular polarization, $\phi_y = \pi/3$ and $\phi_y = 5\pi/12$ are elliptical and $\phi_y = \pi/2$ has linear polarization.

For calculations used monocycle condition as:

A	ω	$FWHM$	ϕ_x	ϕ_y
-4.44	1.0	1.0	$3\pi/4$	$\pi/4$
-3.625	1.0	1.0	$2\pi/3$	$\pi/3$
-3.25	1.0	1.0	$7\pi/12$	$5\pi/12$
-3.14	1.0	1.0	$\pi/2$	$\pi/2$

Table 1: Pulse parameters

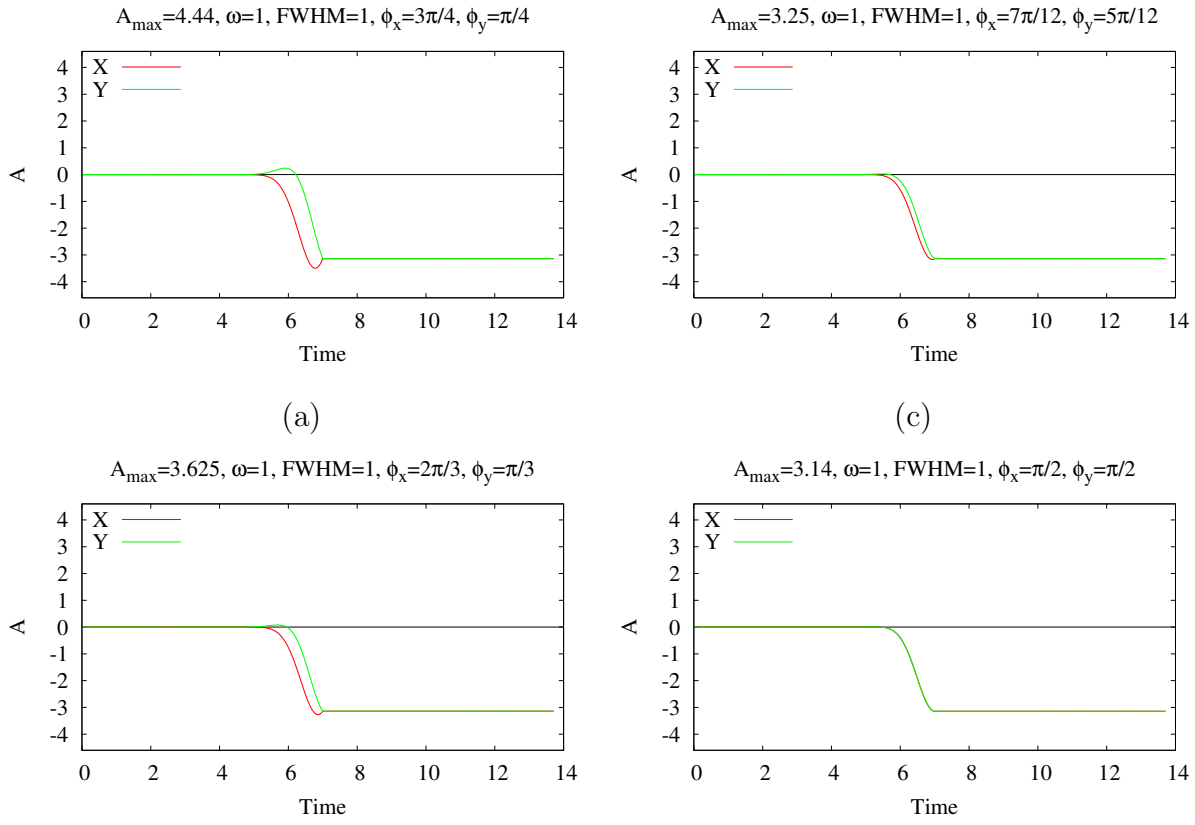

(a) (c)

(b) (d)

Figure 12: Vector potentials.

$$FWHM = \frac{1}{\omega} \tag{2}$$

were FWHM - full width at half maximum, ω - frequency.

To obtain a larger population inversion, it better to apply the pulse with linear polarization; this can be seen from the graph of total energy in Figure 14a. With a gradual increase in polarization from linear to circular, the final value of the total energy decreases slightly. But double occupancy (Figure 14b) almost does not depend on the phase between the X and Y components of the field.

1.2.2 The frequency dependence of the circular π-pulse

Now we look at how the physical parameters of the model change under the action of half-cycle circularly polarized vector potentials with different frequencies. Figure 15 shows the graphs vector potentials for this cases.

Pulse parameters are written in the Table 2.

As shown in Figure 16, the trajectory of the momentum distribution is the same everywhere. But the frequencies are different, which means the higher the frequency, the

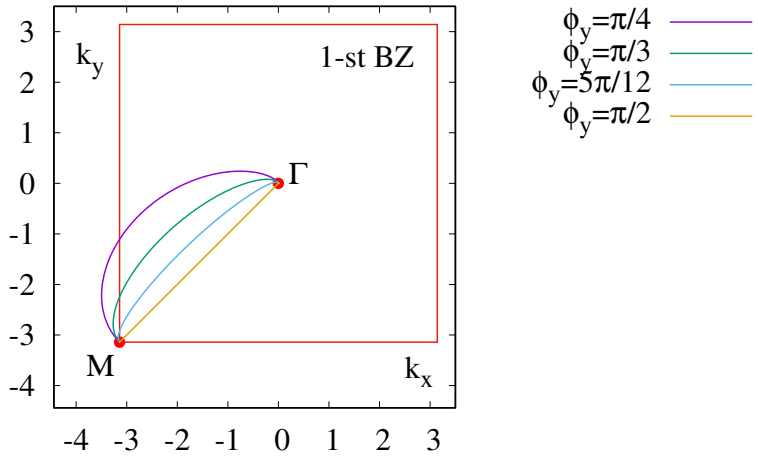

Figure 13: Middle point trajectories of the momentum distribution.

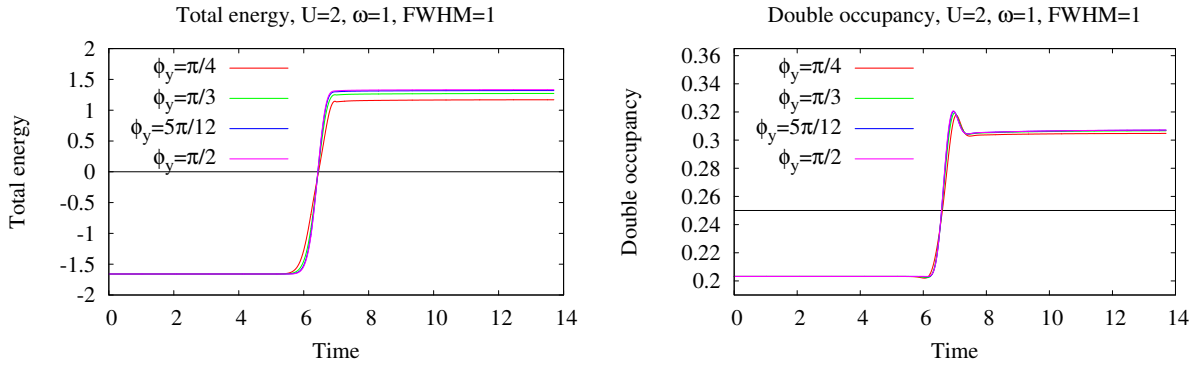

(a) (b)

Figure 14: Total energy and double occupancy.

A	ω	$FWHM$	ϕ_x	ϕ_y
-4.44	0.25	4.0	$3\pi/4$	$\pi/4$
-4.44	0.5	2.0	$3\pi/4$	$\pi/4$
-4.44	1.0	1.0	$3\pi/4$	$\pi/4$
-4.44	1.5	0.667	$3\pi/4$	$\pi/4$
-4.44	2.0	0.5	$3\pi/4$	$\pi/4$
-4.44	16.0	0.0625	$3\pi/4$	$\pi/4$

Table 2: Pulse parameters

faster the momentum distribution will move from the Γ point of the Brillouin zone to M.

Total energy and double occupancy responds strongly to such a frequency change. In Figure 17 it can be seen that the higher the frequency of the pulse, the greater the total energy and double population, and therefore the greater the population inversion.

As example, in Figure 18 depicted the behavior of the momentum distribution in the circular field at different points in time for $U = 2$. The shape of the vector potential for the figure 18 corresponds to figure 15c. Distribution graphs move in the direction of the vector potential at $Time$ =5.0 to $Time$ =7.0 because electric field switched on (Figures 18a-d). After $Time$ =7.0 proses of relaxation start, distribution stop moving and until $Time$ =10.0 topology become more smoother.

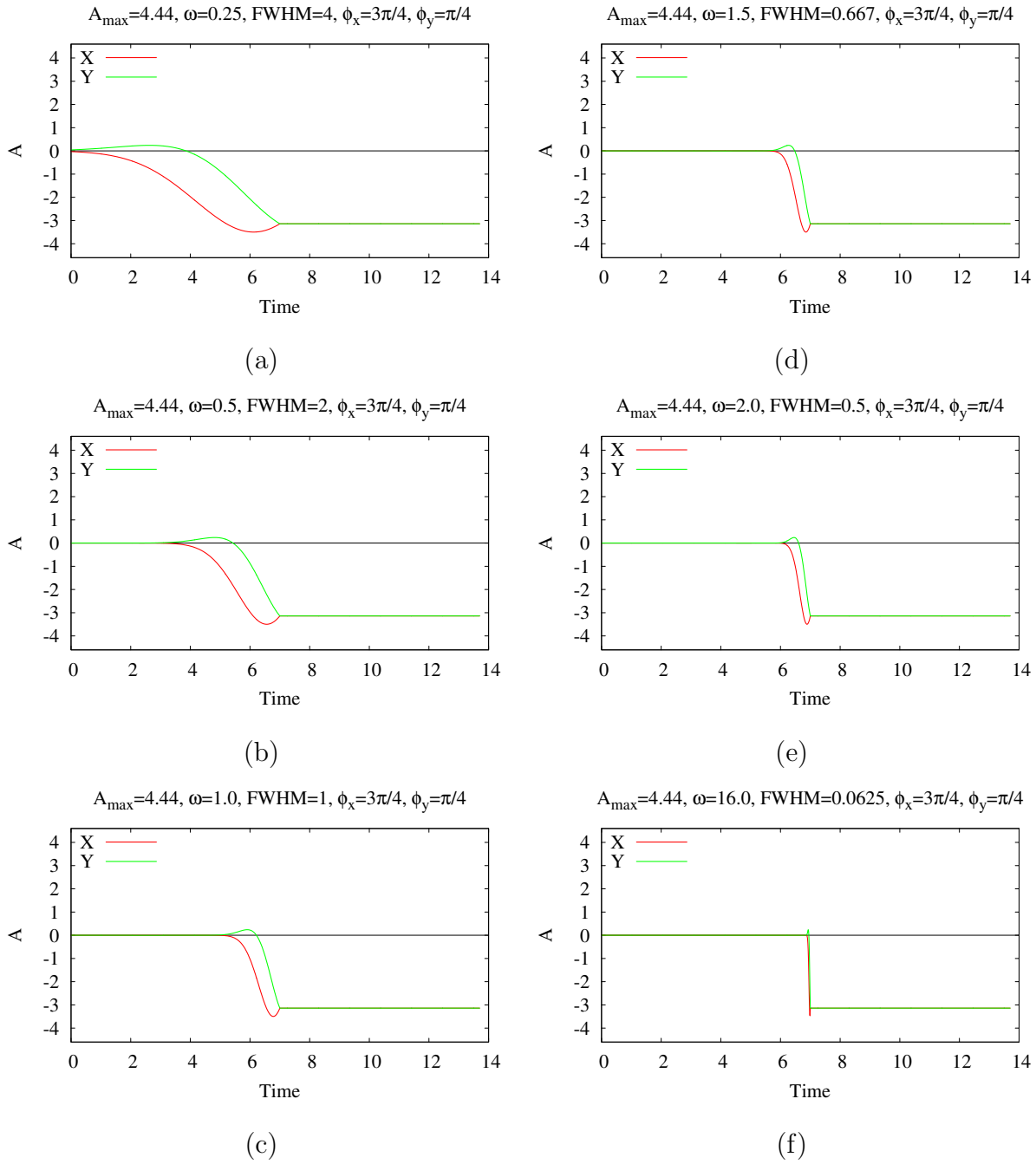

Figure 15: Vector potentials.

1.2.3 Circular monocycle pulse with different initial phases.

Let us proceed to consider how the properties of the Hubbard model change under the influence of monosycle pulses taken at different values of the initial phase (Figure 19).

Pulse parameters are written in the Table 3. Phase for the vector potential in Y-direction taken as initial.

Moving the maximum of the momentum distribution, which was originally located at the Γ point of the Brillouin zone to the M point as depicted in the Figure 20.

The Figure 21 shows the total energy and double occupancy for different values of the initial phases of the vector potential and for various Coulomb interactions. Figure 21a depicts the total energy for a pulse at zero Coulomb interaction. The maximum value of the total energy is reached for $\phi_y = \pi/4$. Total energys for $\phi_y = \pi/6$ and $\phi_y = \pi/3$ are symmetrical relative to the middle of the pulse ($t = 7$) and graph for $\phi_y = 0$ symmetrical itself since it is always equidistant from M points of the Brillouin zone during the whole

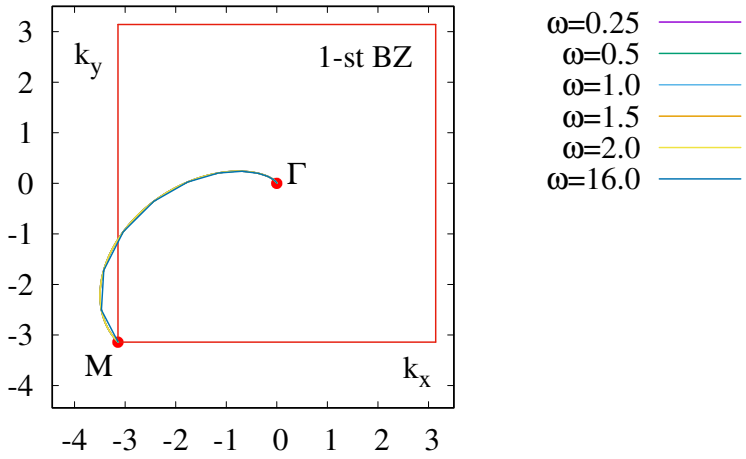

Figure 16: Middle point trajectories of the momentum distribution.

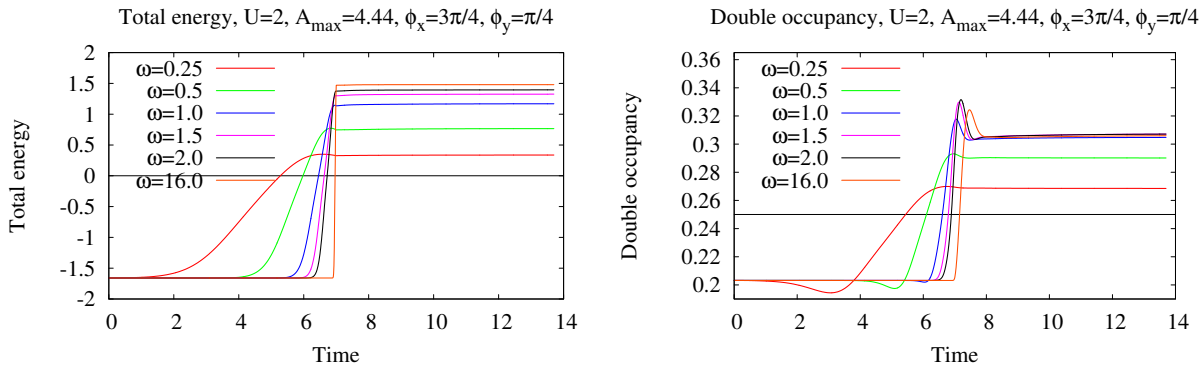

(a) (b)

Figure 17: Total energy and double occupancy.

A	ω	$FWHM$	ϕ_x	ϕ_y
-4.44	1.0	1.0	$\pi/2$	0
-4.44	1.0	1.0	$2\pi/3$	$\pi/6$
-4.44	1.0	1.0	$3\pi/4$	$\pi/4$
-4.44	1.0	1.0	$5\pi/6$	$\pi/3$

Table 3: Pulse parameters

pulse time (Figure 20 red line). Double occupancy (Figure 21a) is equal 0.25 during all time, which must be in case of $U = 0$.

Depending on the magnitude of interaction, symmetry with respect to the middle of the pulse disappears gradually. Figures 21a and 21b show the total energy and double occupancy for a monocycle pulse at different initial phases in the case of $U = 2$. All the considered pulses in one way or another lead to population inversion. Total energys for $\phi_y = \pi/6$ and $\phi_y = \pi/3$ are not any more symmetrical relative to the middle of pulse $t = 7$. Curve at $\phi_y = \pi/6$ has bigger maximum of total energy compare to $\phi_y = \pi/3$. It seems that increasing the interaction increases the absorption of energy by the system and thus increases the temperature during a pulse. The temperature rise makes a flatter momentum distribution that reduces the value of the population inversion, because more electrons are now may extend to the edges of "hat" of the momentum distribution. At the same time,

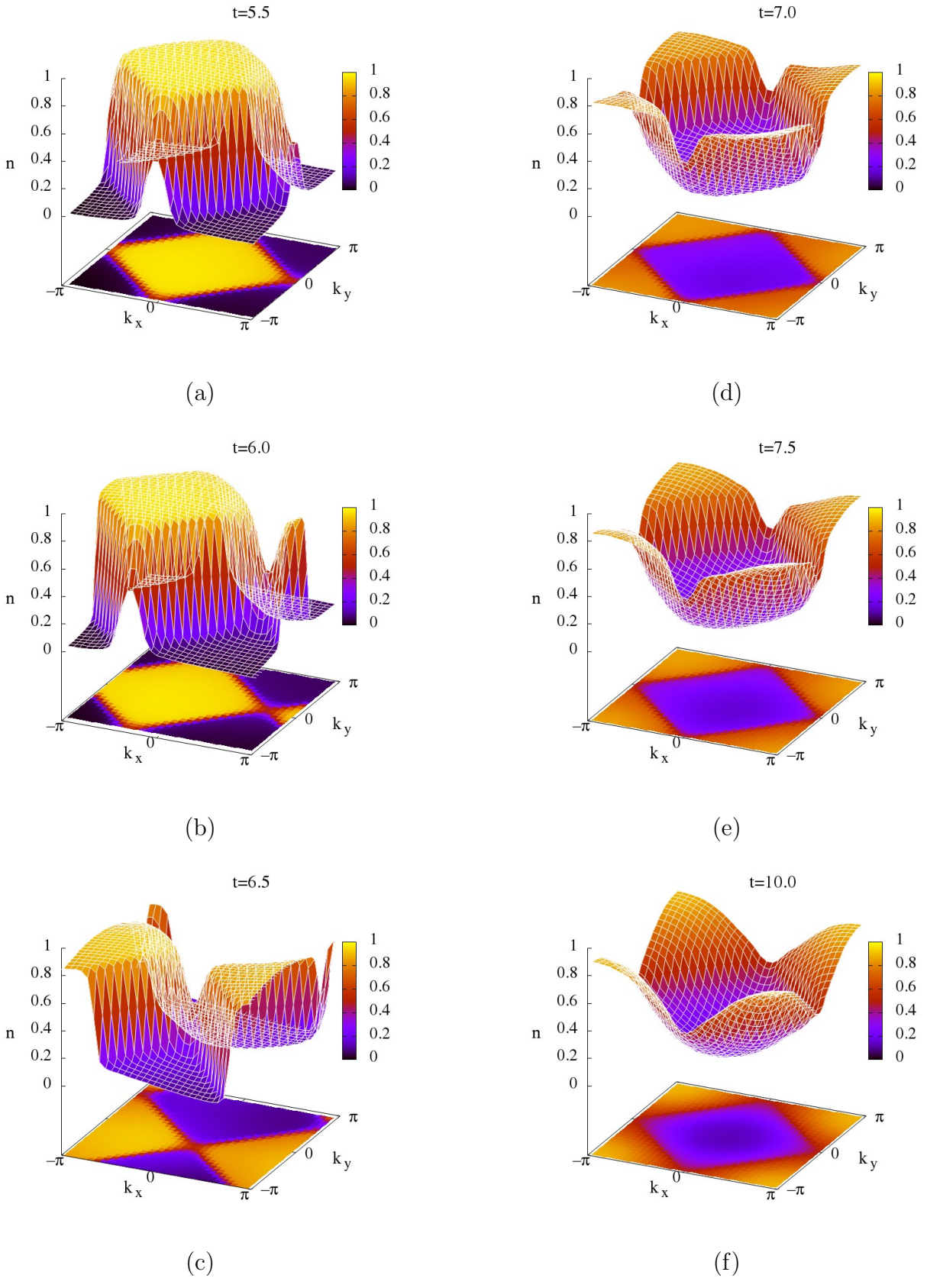

Figure 18: Momentum distribution for pulse with ω=1, FWHM=1.

as shown by previous calculations, the form of the "hat" of the momentum distribution for a correlated system itself may vary during the pulse. Thus, competition of the effects: the inclusion of correlations that tend to bend the "hat" of the momentum distribution, shifting the momentum distribution by the vector potential to a more favorable position and heating the system, may explain why we see the maximum value of the total energy

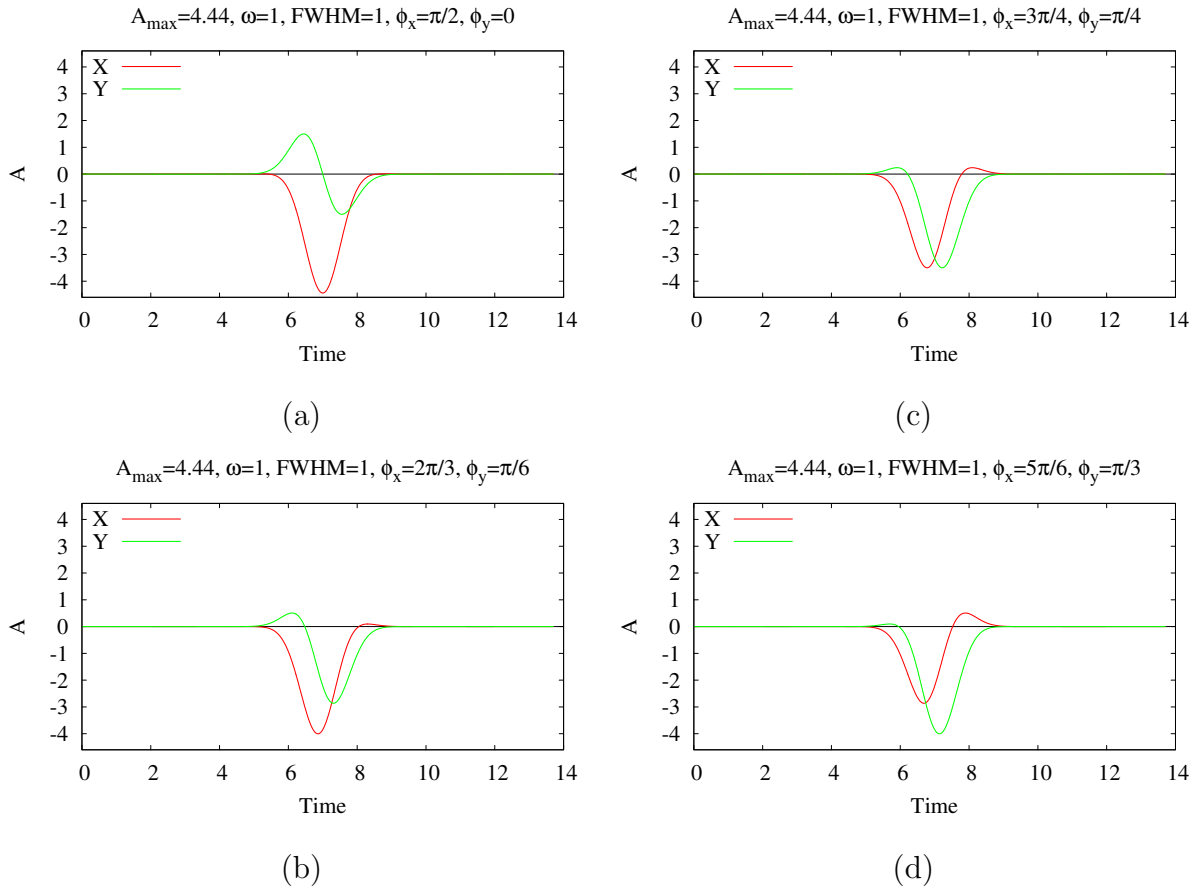

Figure 19: Vector potentials.

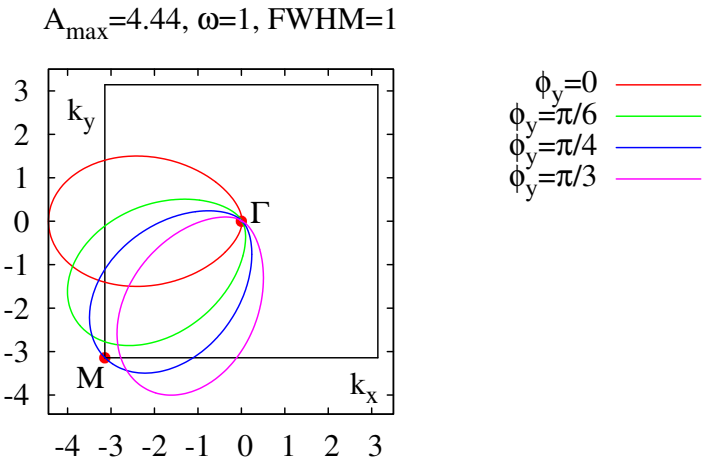

Figure 20: Middle point trajectories of the momentum distribution.

and double occupancy for the pulse with $\phi_y = \pi/3$ slightly larger than for $\phi_y = \pi/4$ in Figure 21b,d.

1.2.4 Away from monocycle condition for π-pulse.

It is interesting to explore how the model behaves outside of monocycle condition. Figure 22 shows the graphs of half-cycle circularly polarized vector potentials with different ratios FWHM and ω.

Pulse parameters are written in the Table 4. By increasing the frequency of pulse

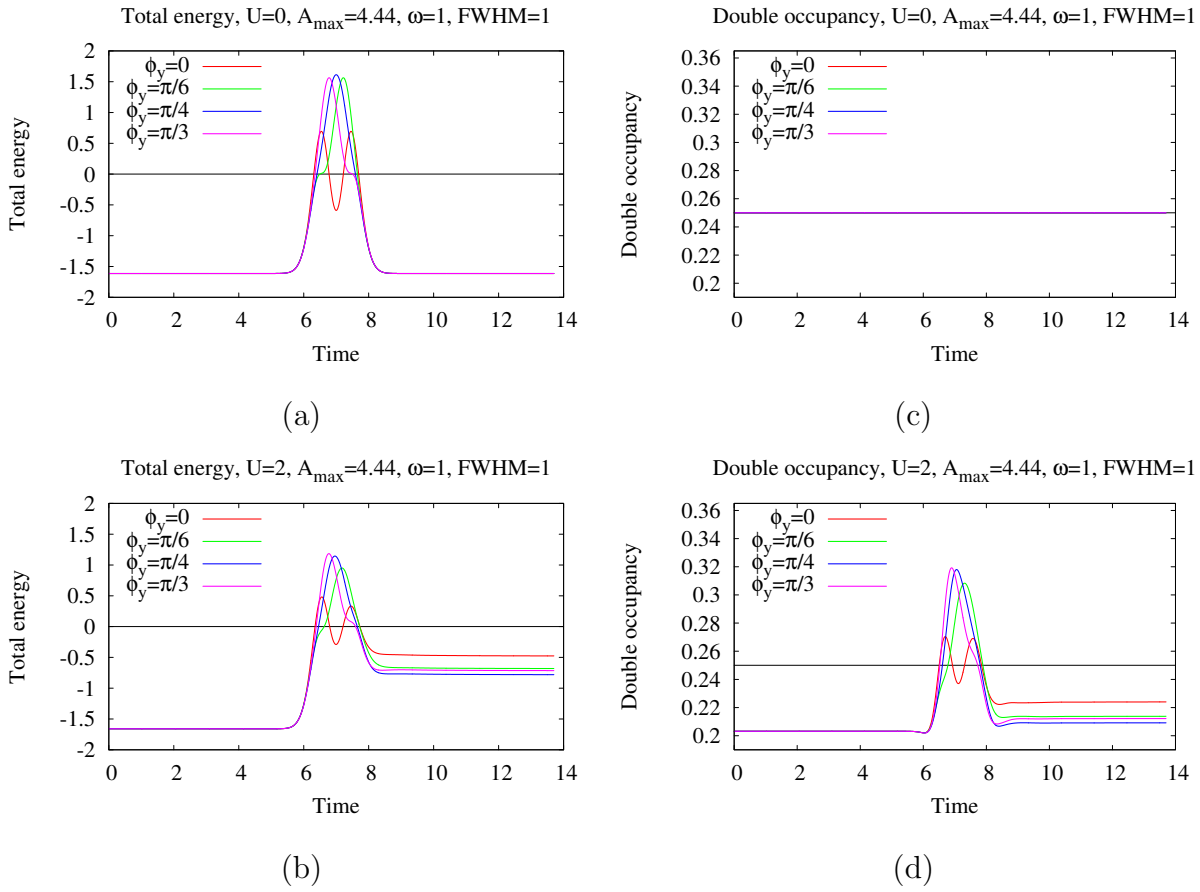

Figure 21: Total energy and double occupancy.

and leaving the FWHM constant, we move away from the monocycle condition Eq.(2).

Figure 23 illustrate trajectory of the center momentum distribution for π-pulse. Line with ω=1 is half-cycle pulse with monocycle condition.

A	ω	$FWHM$	ϕ_x	ϕ_y
-4.44	1.0	1.0	$3\pi/4$	$\pi/4$
-4.44	2.0	1.0	$3\pi/4$	$\pi/4$
-4.44	3.0	1.0	$3\pi/4$	$\pi/4$
-4.44	4.0	1.0	$3\pi/4$	$\pi/4$

Table 4: Pulse parameters

The total energy of such pulses (Figure 24) has a different structure during the excitation, nevertheless optimal inversion presented the π-pulse with monocycle condition. This can be explained by the fact that monocycle condition have shortest way to move center of momentum distribution from Γ to M point, which contributes to less heating of the system.

Leaving the Eq. (2) condition on the graph of the total energy appears peak. Peak gradiently increases and moves towards greater times. Presence of the peak at the total energy is due to fact that the center of momentum distribution in non-monocycle case passes near another M point in the first Brillouin zone, thereby creating an inversion on that part of the trajectory.

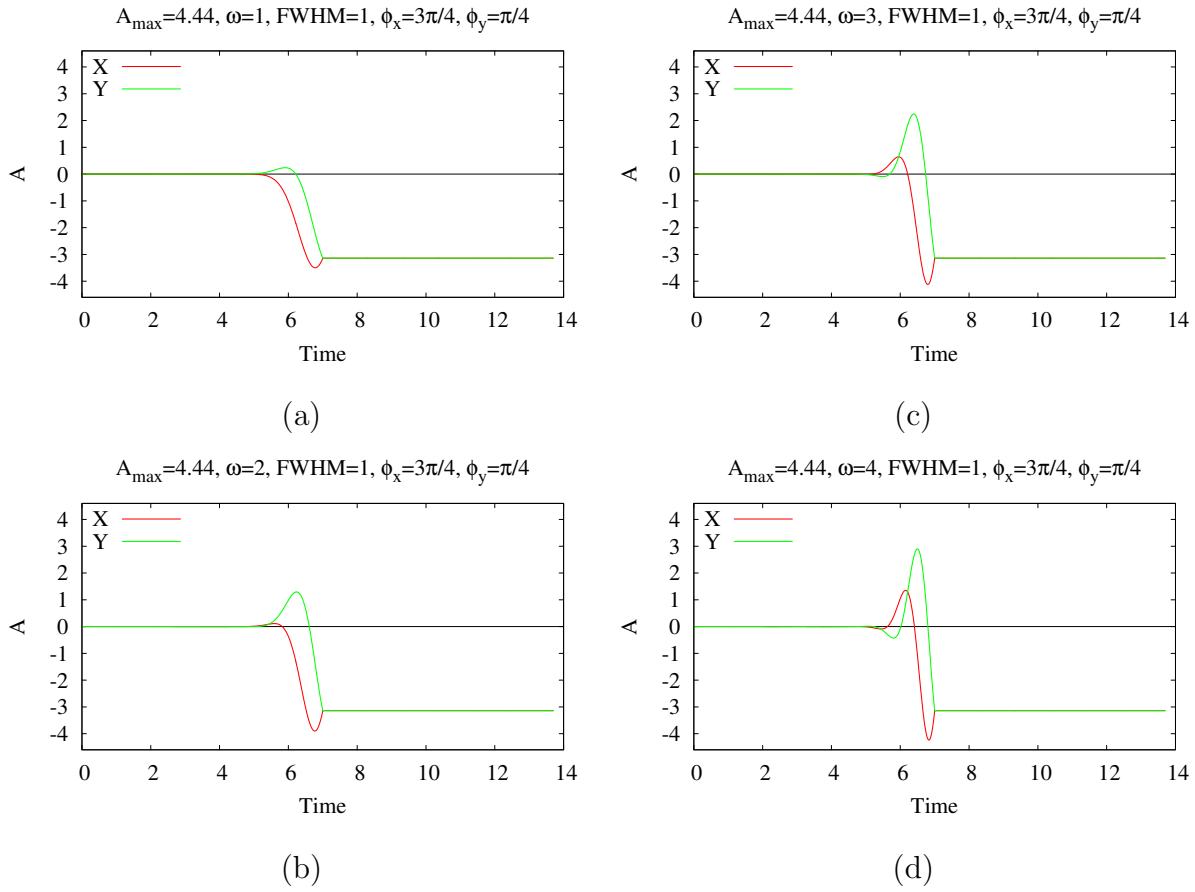

Figure 22: Vector potentials.

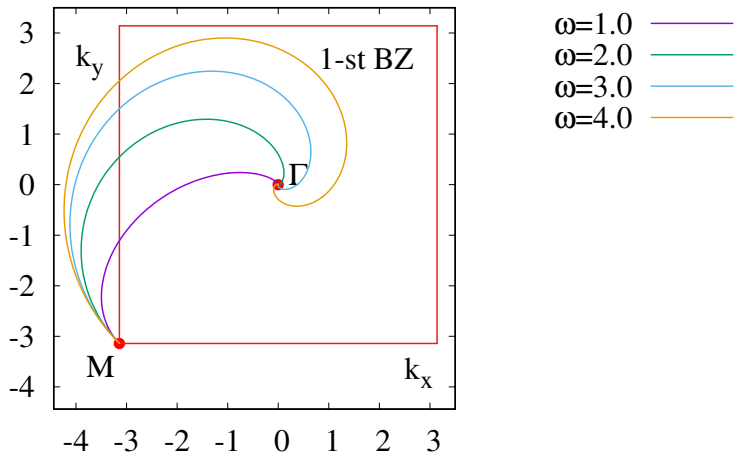

Figure 23: Middle point trajectories of the momentum distribution.

1.2.5 Multicycle pulse.

In this part, we discuss how to create a maximum population inversion during multicycle circularly polarized pulse. Vector potential depicted in Figure 25 has a ramp at the beginning and end, the rest of the pulse has the same amplitude. The maximum amplitude of the vector potential is 4.44.

This form of vector potentialthat move the middle of the momentum distribution from Γ through all four M points in the 2d square lattice Brillouin zone (Figure 26).

The corresponding total energy is shown in Figure 27. Results for all frequencies are

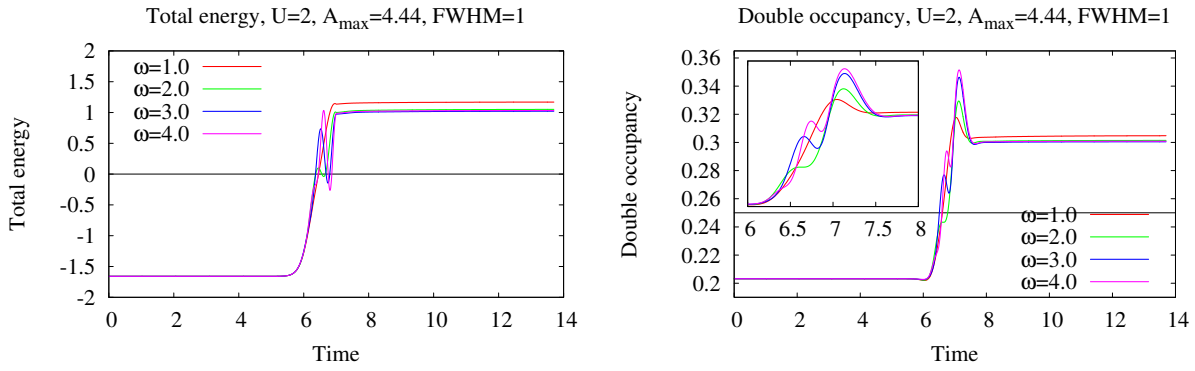

(a) (d)

Figure 24: Total energy and double occupancy.

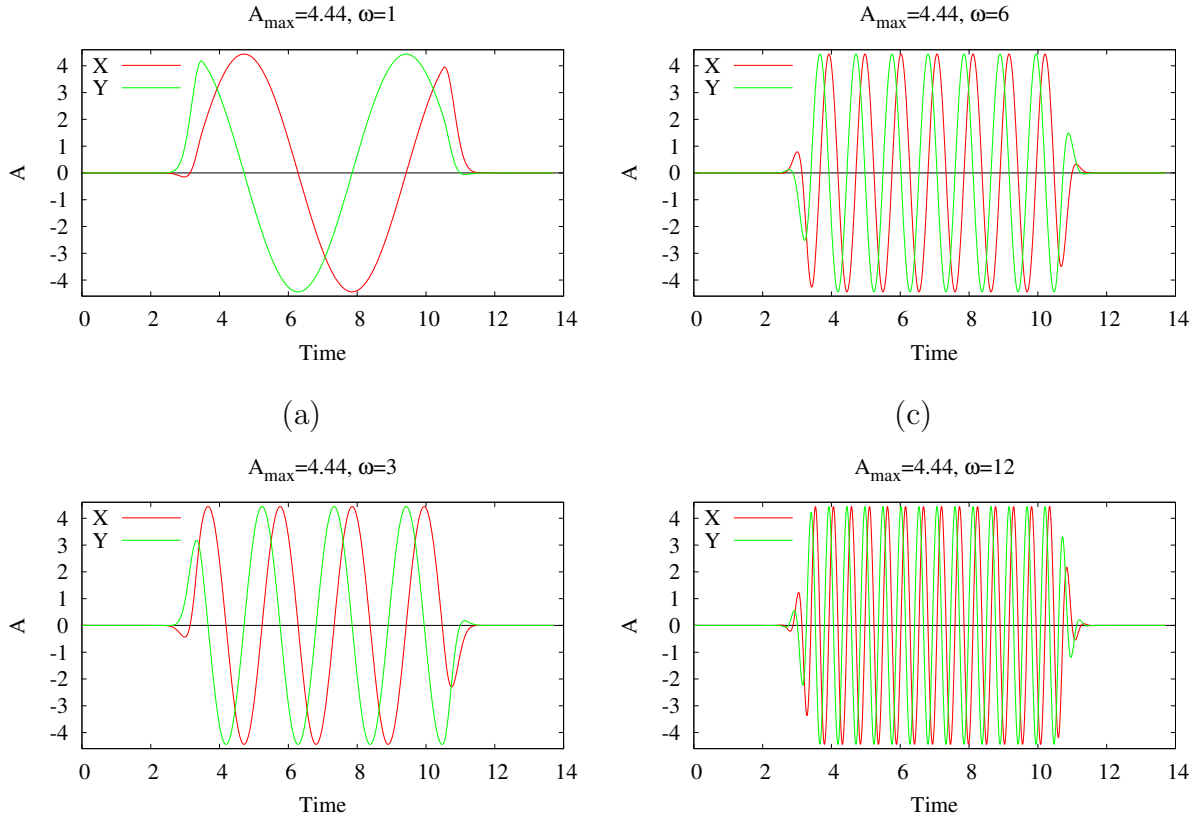

(a) (c)

(b) (d)

Figure 25: Vector potentials.

characterized by general patterns. Initially, the total energy increases from negative to positive value, then oscillates and finally decreases to negative. The behavior of the double occupancy is very similar, except that it can only be positive and grows to a higher value than 0.25. This corresponds to the fact that the maximum of the momentum distribution first goes from the Γ point to a circle close to the M point (Figure 26). Then, moving in a circle near all four M points invertion of the population occurs and over X and Y points in BZ it sometimes disappears. And finally, at the end of the pulse, the maximum of distribution returns to its initial location at the Γ point, but already changed by the effects of correlations and the external field.

As the field frequency increases, the total energy tends to oscillate and be in the majority with a positive value than higher the field frequency, the longer it remains in

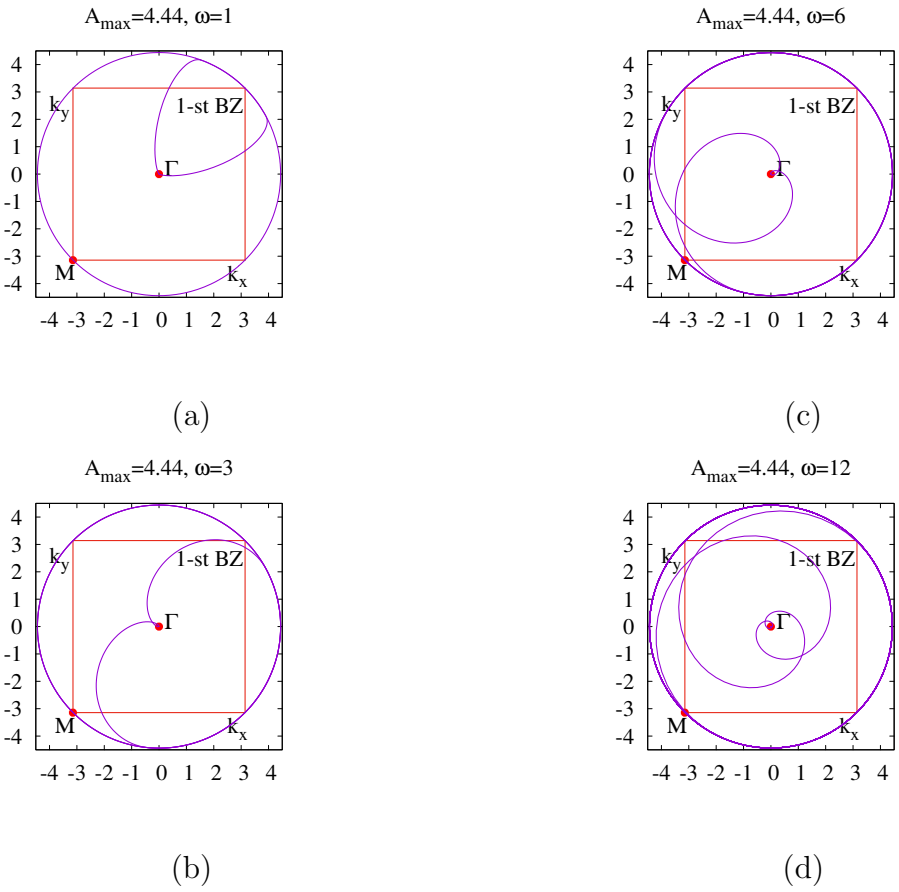

Figure 26: Middle point trajectories of the momentum distribution.

this range. The double occupancy fully arrives above 0.25 at the time of the exitations for frequencies above ω=1.

It should also be noted that the total energy and double occupancy at high frequencies of the external field initially have a change in the amplitude of oscillations, but after some action of the exitation, the mean value and amplitude of oscillations hardly change. This implies that we detect a transition to Floquet mode where physical observables are periodic in time.

Thus, summarizing the various options for changing the sign of the interaction in the Hubbard model under the influence of a circular field, we select several conclusions:

1. Creating of the population inversion becomes more efficient in linear pulse compare to circularly polarized (Figure 14a).

2. Higher pulse frequency helps to significantly increase inversion in the circulary polarized π-pulse (Figure 17).

3. With a circular vector potential, the maximum positive value of the total energy depends on the initial phase as well. To create maxim of population inversion, interesting is that it is not necessary to have a phase due to which the middle of momentum distribution is transferred exactly from the Γ point to M, as previously expected. This case is shown in the Figure 21b.

4. Move away from monocycle conditions allows to create controlled peaks of total energy that can change the sign of the interaction even under the condition of a half-cycle electric field (Figure 24a).

5. For stable population inversion in the Floquet mode, it is necessary to apply a high-frequency field which is capable of moving the maximum of momentum distribution near the corners of the first Brillouin zone (Figure 26).

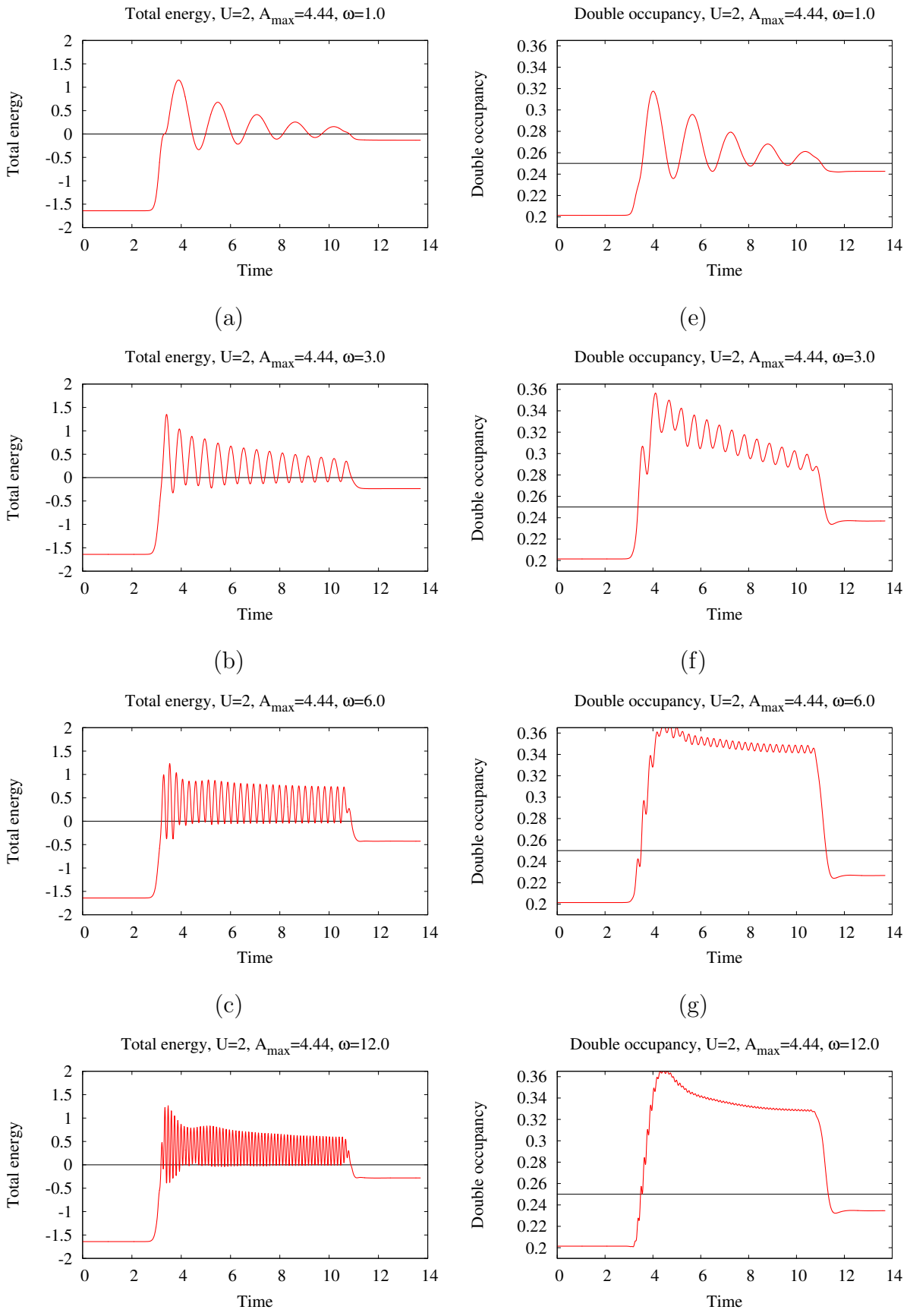

Figure 27: Total energy and double occupancy.

References

N. Tsuji, T. Oka, H. Aoki, and P. Werner. Repulsion-to-attraction transition in correlated electron systems triggered by a monocycle pulse. *Phys. Rev. B*, 85:155124, Apr 2012. doi: 10.1103/PhysRevB.85.155124. URL https://link.aps.org/doi/10.1103/PhysRevB.85.155124.